Heliyon 8 (2022) e10696

Contents lists available at ScienceDirect

Heliyon

journal homepage: www.cell.com/heliyon

Research article

Spatiotemporal land use and cover changes across agroecologies and slope gradients using geospatial technologies in Zoa watershed, Southwest Ethiopia

Ginjo Gitima [a,*], Menberu Teshome [b], Meseret Kassie [a], Monika Jakubus [c]

[a] Department of Geography and Environmental Studies, University of Gondar, P. O. Box 196, Gondar, Ethiopia
[b] Department of Geography and Environmental Studies, Debre Tabor University, P. O. Box 272, Debre Tabor, Ethiopia
[c] Department of Soil Science and Microbiology, Poznan University of Life Sciences, ul. Szydłowska 50, 60-656, Poznan, Poland

ARTICLE INFO

Keywords:
Land use land cover
Drivers
Agro-ecologies
Slope gradients
Socioeconomic analysis

ABSTRACT

Environmental phenomena are always changing elsewhere in various scales depending on both natural phenomenon and human interference. Land use/over change (LULC) is related to site specific factors such as inappropriate land use planning and the expansion of traditional agricultural practices in steep gradients have led to soil erosion and consequent ecological changes. Thus, it is crucial to determine the trend, pattern, and drivers of land use/land cover dynamics for sustainable natural resource management in Ethiopia. Therefore, we evaluated the spatio-temporal LULC dynamics in different agroeclogies and slope gradients, and their drivers between 1985 and 2021 in the Zoa watershed of Omo-Gibe basin, Southwest Ethiopia. Landsat imageries, focus group discussants, key informants, and field observations were used as source of data to analyze the spatio-temporal LULC trajectories and their drivers. With total accuracies ranging from 87.55% to 91.14%, supervised image classification using the Maximum Likelihood classifier technique was used to categorize five key LULC classes: bareland, farmland, forestland, grassland, and shrubland. The results revealed that shrubland (41.87%) had the largest share in 1985, but later declined to 23.98% in 2000, and 12.6% in 2021. Grassland has declined as well, from 17.15% in 1985 to 2.09% in 2021. In contrast, farmland increased at the fastest rate, from 29.09% in 1985 to 71.12% in 2021. The proportion of farmland exhibited an increasing trend in all agro-ecologies, while forestland has increased only in highland agro-ecologies. Between 1985 and 2021, an extensive area of shrubland and grassland were converted into farmland with a conversation rate of 1.05% and 0.58% per annum, respectively. The expansion of farmland was observed towards moderately and steep rolling slopes which might exacerbate soil degradation. This is due to rapid population increase and ongoing demand for agricultural land. The result of key informant interviews and focus group discussions also revealed that expansion of farmland and settlement are the major drivers of LULC dynamics due to rapid human population growth. Therefore, the regional government and various stakeholders should work on redesigning effective management strategies through appropriate land use planning to address the adverse effects of LULC dynamics.

1. Introduction

Land is a vital natural resource with several natural, social, and economic applications (Hailu et al., 2020). Land use denotes how humans use the land for various activities while land cover indicates the biophysical attributes, which are of either natural and/or human origin, covering the earth's surface (Jansen, 2010). LULC refers to both due to natural and anthropogenic changes to land resources (Jacob et al., 2015; Kidane et al., 2019; Tolessa et al., 2020). According to Regasa et al. (2021), LULC analysis is amongst the most typically used techniques for determining how the land has been utilized in the previous time, what varieties of investigations are expected to be conducted in the future, and the causes and processes that are driving these changes.

Unmanageable changes in LULC are serious environmental challenges in various regions of the world (Gashaw et al., 2017). The impacts of LULC change have been linked at various scales including land degradation, changes in biodiversity, intensification of climate change from a global perspective (Omran, 2012) increased sedimentation of stream

* Corresponding author.
E-mail address: ginjo.gitimo@bongau.edu.et (G. Gitima).

https://doi.org/10.1016/j.heliyon.2022.e10696
Received 5 April 2022; Received in revised form 17 June 2022; Accepted 14 September 2022

courses, changed land-atmospheric interaction patterns that may alter the weather and climatic variability, and carbon balances at regional scales (Auch et al., 2022). Local impacts include severe land resource disruptions (Haregeweyn et al., 2015; Berihun et al., 2019; Degife et al., 2019) upsurges soil erosion (Kidane et al., 2019), wetland shrinkage, and declines in water quality (Xu et al., 2019) and diminishes sustainable ecosystem services from agriculture (Hussain et al., 2022; Xu et al., 2022). In contrast, the livelihoods of poor people are adversely disrupted since they rely on land and natural resources due to expansions of cultivated and grazing land turned into forests and grasslands in the world (Lambin et al., 2003; Nkonya et al., 2012, 2016). In addition, global cropland area increased by 11.5% between the 2000–2003 and 2016–2019 interval, and its largest net was increased in Africa, followed by Asia and South America (Potapov et al., 2022). Similarly, agriculture has increased by 57%, while the country has lost 5% of its woodland and pasture land, and 16% of its forest acreage between 1975 and 2000 in Africa and more than 50,000 km^2 of natural vegetation has been lost per year (Eva et al., 2006). The upsurge was basically intense with a decrease in forest, bushlands, and grasslands in the Horn of Africa (Measho et al., 2020). However, the directions, rates and intensities of LULC changes in each land use type were not uniform in all parts of the world (MEA, 2003; Haregeweyn et al., 2015; Gashaw et al., 2017).

Ethiopia has experienced very rapid LULC changes due to human-induced drivers like resettlement programs and population pressure as well as natural-induced driving forces like the variability of climate change, slope inclinations and agroecological categories (Regasa et al., 2021). LULC change associated with land degradation processes is currently increasing at an alarming rate, contributing a significantly large amounts of soil loss. This is especially true in Ethiopia, where agriculture is the pillar of the country's economy (Berihun et al., 2019). Recent LULC change studies in various areas of the country observed disparate trends through the increase of cropland at the detriment of forestland in many areas (Gashaw et al., 2017; Minta et al., 2018; Betru et al., 2019; Degife et al., 2019; Gessesse et al., 2019; Habte et al., 2021; Ogato et al., 2021). However, an increasing trend in forest areas was detected due to new plantation sites on degraded hill slopes in few areas of the countryside (Bantider et al., 2011; Gebrelibanos and Assen, 2015; Nigussie et al., 2016).

Spatio-temporal pattern of LULC changes is triggered by both biophysical and anthropogenic driving factors in various parts of Ethiopia ((Betru et al., 2019; Degife et al., 2019; Aneseyee et al., 2020; Dibaba et al., 2020; Sisay et al., 2021). Biophysical factors, including slope categories and agroecologies, have a significant impact on LULC extents, particularly the rate and process of deforestation (Hishe et al., 2015). These factors determine the heterogeneity of vegetation, climatic conditions, and land cover types concerning socio-economic drivers (Birhane et al., 2019). Moreover, the drivers of LULC trajectories are dynamic, and they vary across counties depending on the social, economic, biophysical, and political factors (Yesuph and Dagnew, 2019; Dibaba et al., 2020; Ewunetu et al., 2021; Ogato et al., 2021). However, driving factors of LULC changes vary through time and space based on the country's distinct human-environment characteristics (Kindu et al., 2015; Hailemariam et al., 2016; Belay and Mengistu, 2019; Dibaba et al., 2020; Hailu et al., 2020; Tolessa et al., 2020; Ogato et al., 2021). For instance, Berihun et al. (2019) found that growth in population and shifting farming techniques (e.g., cultivation of A. decurrens plantation) are the primary drivers of LULC changes in western Ethiopia. On other hand, Betru et al. (2019) found that small-scale subsistence and large-scale commercial agriculture are the primary proximal drivers of LULC dynamics. In addition (Degife et al., 2019), and (Ogato et al., 2021) studies in Ethiopia's Lake Hawassa and Huluka watersheds, respectively, outlined biophysical factors, agricultural expansion, infrastructure and urban expansion, forest clearing, fast human population growth, rapid technology, and land tenure system are the major drivers of the LULC changes.

Different scholars have studied spatiotemporal LULC dynamics in various parts of Ethiopia (Belay and Mengistu, 2019; Betru et al., 2019; Degife et al., 2019; Gessesse et al., 2019; Hailu et al., 2020; Hishe et al., 2020; Tolessa et al., 2020; Ogato et al., 2021; Sisay et al., 2021). Most of these researchers found that LULC dynamics vary across the country in terms of pattern, direction, and magnitude. However, most of the aforementioned studies missed considering LULC dynamics across agro-ecological zones and slope gradients concerning specific LULC classes. In addition, the majority of these studies took place outside of the research field. Moreover, the findings were contradictory, possible due to heterogeneity in natural resource distribution, monitoring, and management systems (Ewunetu et al., 2021). The discrepancy in results could be related to a variety of socioeconomic shifts as well as biophysical factors such as agro-ecologies and rolling of slopes (Birhane et al., 2019; Belay and Mengistu, 2019). Since Ethiopia experiences diverse agro-ecologies, various slope categories and socioeconomic dynamics (Ewunetu et al., 2021), timely site-specific study by integrating remote sensing data with information from local land users can provide more insight on LULC changes and their drivers of change for making sustainable natural resource management decisions in the study area.

Zoa watershed is an important part of Gibe-III hydroelectric dam within Omo-Gibe basin. However, in comparison to other parts of Ethiopia, the watershed lacks multidisciplinary and independent research. Understanding the spatiotemporal trajectories and patterns of LULC changes in the context of a larger socio-ecological scheme and slope gradients at the watershed level assists in comparing different portions of the watershed and identifying those that are vulnerable to change (Dibaba et al., 2020). In addition, investigating the dynamics of LULC is an ever more important issue in the study of environmental alteration to evaluate and determine the current state of resources and planning choices for long-term resource management. Therefore, as part of this research, the following particular objectives were determined (i) to assess the spatio-temporal LULC trajectories in Zoa watershed of Omo-Gibe basin over the periods of 1985 and 2021 with special attention to agro-ecological zones and slope gradients. (ii) To evaluate the major drivers of LULC dynamics in the study area using among other things socioeconomic analysis.

2. Methods and materials

2.1. Study area description

This study was conducted in Zoa watershed of Omo-Gibe basin, which is located in the Northwestern part of Dawuro zone, Southwest Ethiopia. Astronomically, the watershed lies from 7°3′00″-7°15′00″N Latitude and 37°2′00″E-37°23′00″E Longitude within the Omo-Gibe basin (Figure 1). It extends across five districts (Maraka, Tarcha Zuria, Gena, Zaba Gazo, and Loma Bossa) of southwest Ethiopia at a distance of about 490 km from Addis Ababa, the capital city of Ethiopia across Butajira-Hosana road and 520 km through Jimma via Tarcha Road. The elevation of Zoa watershed varies from 914 to 3011 m above sea level (Figure 1). The watershed covers a total area of 599.018 square kilometers.

According to the MOA Ministry of Agriculture, 1998 classifications, the agro-ecologies of the Zoa watershed are categorized as 28.43% is lowland (*Kola*), with elevations ranging from 914 to 1500 m above sea level, and 63.91% is midland (*Woinadega*), with elevations ranging from 1500 to 2300 m above sea level. The remaining 7.65% is classified as highland (*Dega*) with an elevation of more than 2300 m above sea level (Figure 2a).

Similar to other parts of the Dawuro zone, the topographic feature of the Zoa watershed is diverse, which varies from an undulating landscape to an extended, steep slope escarpment and mountains. It is characterized mainly by strongly sloping and moderately steep slopes, which make the area highly susceptible to soil erosion hazards. As a result, slope status is one of the characteristics that indicate the pace of soil erosion and, one of the indications of suitability for agricultural activities.

Slope form, steepness, and length influence the level of soil erosion and runoff (Yesuph, 2020). After reclassifying DEM into six FAO (2006)

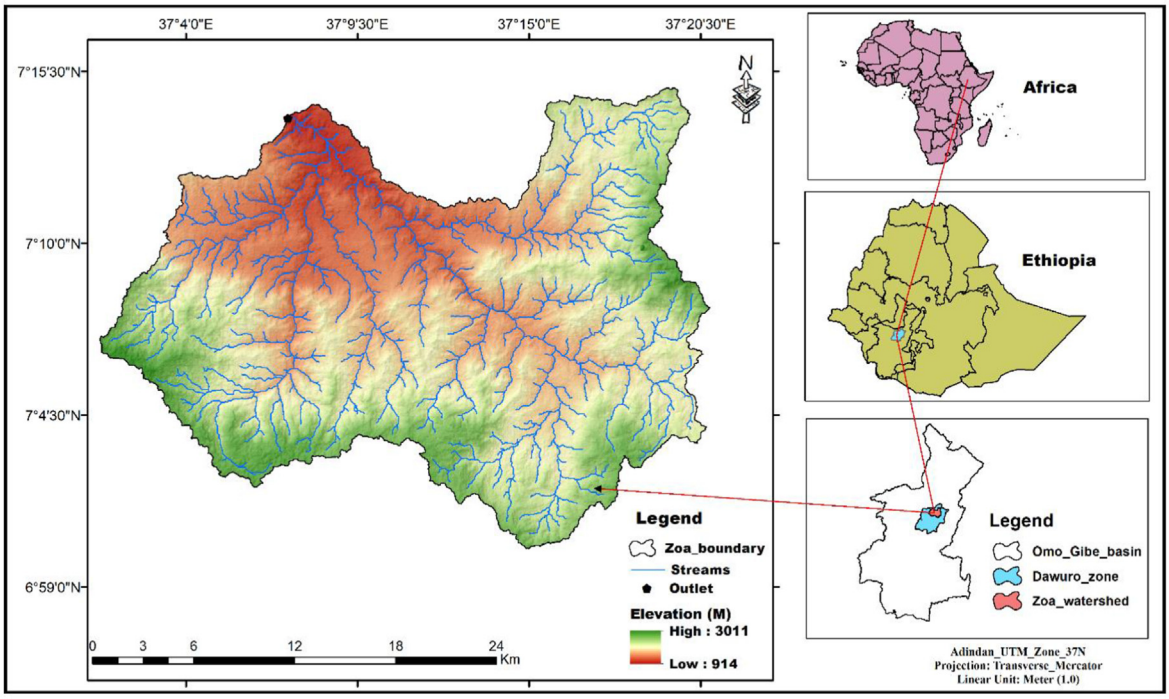

Figure 1. Map of the study area.

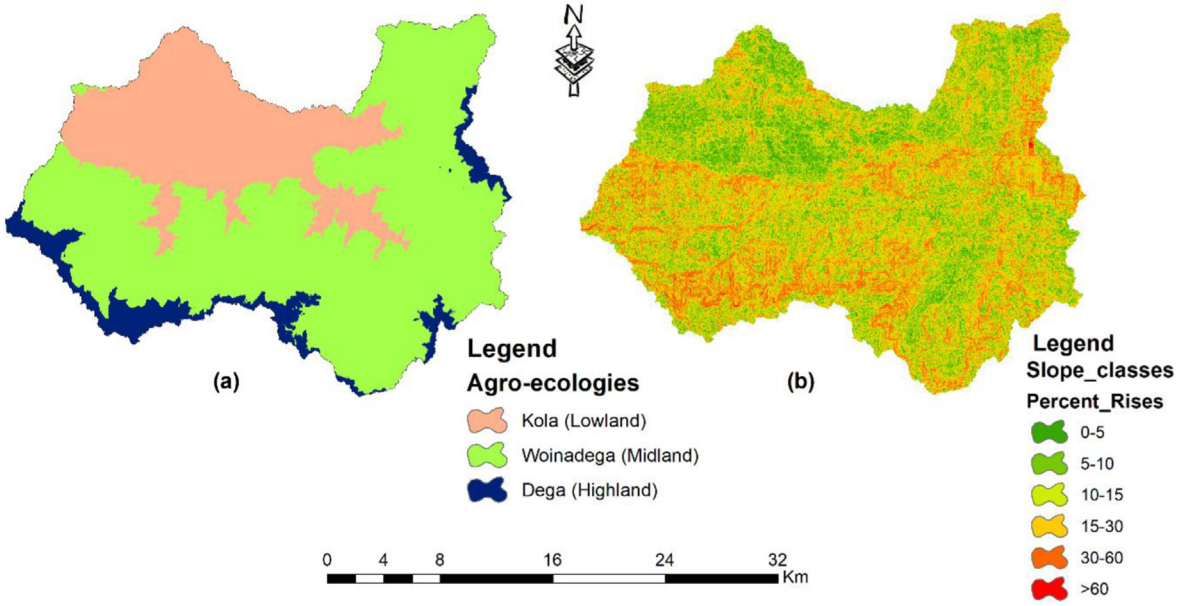

Figure 2. The classifications of agro-ecological zones (a) and slopes (b) of the watershed.

slope classes, 8.85% of the Zoa watershed has flat to gently sloping (0–5), whereas 20.9% and 21.5% of the total areas are categorized as sloping (5–10) and strongly sloping (10–15) slopes, respectively (Figure 2b). The remaining land area is classified as moderately steep (15–30), steep (30–60), and very steep (>60), accounting for 36.58%, 12.02%, and 0.08%, respectively (Figure 2b). In comparison, the northwestern half of the area has a flat to gently sloping landscape with little rugged terrain. On other hand, the southwestern part and eastern margin of the watershed are dominated by rugged terrains, and very steep slopes with high altitudes (Figure 2b).

Zoa watershed exhibits climatic variations from lowland to highland (Gezmu et al., 2021). The watershed receives a total annual rainfall of 1398.8 mm, with mean minimum and maximum annual temperatures ranging from 14.65 °C to 16.12 °C and 26.4 °C–29.3 °C, respectively (Gitima et al., 2021). Temperature becomes intense in January, February and March. The rainfall is a bimodal type in the watershed. March to May is the short rainy season, while June to September is the long rainy season (Gitima et al., 2021). The Zoa river is a tributary of the Omo-Gibe basin that flows from the south east to the northwest, eventually reaching the Gojeb river. Zoa River is permanently flowing with a lesser volume of water during the drier (January to March) months. There is no fishing, irrigation, or recreational usage of the river. The precious topsoil is eroded and contributed to the ever-increasing sediment deposits in Gibe III dam and Zoa river banks.

The majority of societies in the Zoa watershed (over 91 percent) live in rural and rely on a mixed crop-livestock production system for their livelihood (Gezimu et al., 2021). Cultivation of perennial crops is the most common land use in the watershed including enset[1] (*Ensete ventricosum*), coffee (*Coffea arabica*), banana (*Musa acuminate*), mango (*Mangifera indica*), avocado ((*Persea americana*), etc. In contrast, the annual food crops include cereals such as maize (*Zea mays)*, wheat (*Triticum vulgare),* sorghum (*sorghum Bicolor*), teff (*Eragrostis tef*), pulses lentil (*Lens culinaris*), beans (*Phaseolus vulgaris*), peas (*Pisum sativum*), and root crop like yams, potatoes, sweat potatoes and, etc (Gitima and Legesse, 2019). Even though the watershed has a lot of agriculture potential; farmers use traditional means of production results very low productivity. Furthermore, agricultural activity is primarily rain-fed, and market access is limited, rendering farming households' livelihoods extremely stagnant (Gitima et al., 2021). Farmland, grassland, forestland, shrubland, and bareland are among the five major LULC classifications identified in the research area (Table 1).

Table 1. The major LULC classes and their description in the study area.

S. No	LULC classes name	Description
1.	Farmland	The cultivated fields of farm households, as well as the scattered rural villages that are inextricably linked to them. Because it was difficult to distinguish scattered rural settlements as a distinct LULC class in areas with the dispersed farming areas, they were merged into one (Belay and Mengistu, 2019; Ewunetu et al., 2021; Sisay et al., 2021).
2.	Grassland	Areas with temporary grass cover, are usually used for grazing and land units are allocated as a source of animal feed (Belay and Mengistu, 2019; Aneseyee et al., 2020).
3.	Forestland	Area is covered with dense trees, which include both natural and plantation trees, with an area that exceeds 0.5 ha (Sisay et al., 2021).
4.	Shrubland	Area is covered by sparely distributed bush trees and grasses mixed with shrubs (Degife et al., 2019; Aneseyee et al., 2020).
5.	Bareland	Areas with little tree cover and a stony surface alongside the flooding areas of local river valleys, over steep mountainsides and gentle (Ogato et al., 2021).

2.2. Data sources, methods of acquisition and analysis

2.2.1. Remotely sensed data

To delineate the research area boundaries and to compute morphometric characteristics of the watershed, a remotely sensed SRTM-DEM or Shuttle Radar Topographic Mission (30*30m) was downloaded from the United States Geological Survey (USGS). Since 1972, the USGS has provided free Landsat images to monitor changes on the Earth's surface (Turner et al., 2015). As indicated in Table 2, three sets of longitudinal time series satellite images such as Landsat TM (1985), Landsat ETM+ (2000) and Landsat 8 OLI-TIRS (2021) were retrieved from the USGS Earth Explorer (http://earthexplorer.usgs.gov). The year 1985 has been purposefully selected to divide the study periods into three classes such as 1985–2000, 2000–2021 and 1985–2021 images. The year 1985 was taken as a benchmark since the Ethiopian government started the resettlement programs in north, south, and southwestern Ethiopia which might have a significant effect on LULC. The data quality layer indicates the presence of atmospheric contamination including clouds, haze and topographic shadows which determine the accuracy of satellite images. To avoid data inconsistency and gaps in cloudy regions (where only a few clear-sky observations per year are available in the study area during the dry season) we implemented a gap-filling technique. Therefore, all images of data sets were obtained in the dry season (December to February) with the lowest percent or less than 10% cloud cover to increase the accuracy of land use type classifications. Furthermore, secondary data such as a topographic map (scale1:50,000) of the study area was procured from the Ethiopian Geospatial Information Agency (EGIA) to determine georeferencing process for LULC class verifications, training sites, and to verify the quality of the 1985 satellite images. Furthermore, training samples for the year 2000 image reference data using a temporal slider image and for the year 2021 LULC classes and their accuracy assessments were collected using Google Earth data sets.

2.2.2. Socioeconomic and field data

Focus group discussions (FGDs) and key informant interviews (KII) were used to collect socioeconomic data to identify LULC change drivers. Both FGDs and KIIs were selected by using a non-random sampling method that was carried out from November to December 2021 to collect the drivers of LULC dynamics in the watershed. Hence, eight (8) focus group discussions were conducted in eight kebeles with a small number of six to ten farmers as recommended by Marczyk et al. (2005) in each group using a semi-structured checklist. In addition, 45 informants were interviewed, including eight from development agents, five from non-governmental organizations, sixteen model farmers, and sixteen elderly farmers from various communities of the watershed. The key informants were purposively selected for their significant experience, unique insight, and in-depth understanding of the topic under investigation. Moreover, preliminary field data was acquired using GPS from 294 current ground control truth points in the watershed to identify the actual LULC classes.

2.3. Methods of data analysis

To analyze time series datasets of LULC, this study adopted the following methodological stages. (1), image pre-processing, (2) image classification, (3) accuracy assessment, (4) LULC change detection analysis, and (5) socioeconomic data analysis. The study's methodology flowchart is depicted in Figure 3.

2.3.1. Image processing and LULC detection analysis

2.3.1.1. Image pre-processing. Geometric rectification, bad line detection, atmospheric correction, radiometric calibration and topographic correction were all part of the pre-processing procedure (Tewabe and Fentahun, 2020) in this study. Due to solar position and satellite calibration, radiometric and geometric corrections were used to remove sensor noise, haze, corrective data loss, and missed lines (Aneseyee et al., 2020; Abdo and Prakash, 2020). Therefore, all Landsat images of the watershed were projected to the World Geodetic System (WGS_84_UTM_Zone_37N) and corrected geometrically using ground control points. To enhance image quality, atmospheric adjustments such as haze reduction was also prior performed. Furthermore, for radiometric correction, raw DN (digital number) values were transformed into reflectance values. All-time series satellite images were done by using ERDAS Imagine 2014 software and were extracted or subset for covering the watershed territory only.

2.3.1.2. Image classification and accuracy assessment. In this study, we used two important LULC dynamics image classification algorithms. Firstly, an unsupervised classification technique was used to identify the primary LULC classes using the visual interpretation method. Secondly, a supervised classification procedure was preferred for all satellite images to acquire a signature for each LULC class. The main image classifications were done, including visual interpretation of images to identify the major LULC classes using the Maximum Likelihood classification algorithm and change detection comparison techniques. The maximum likelihood classifier is the most extensively used parametric classification technique, and it accounts for the spectrum information of LULC classes using a per-

[1] An herbaceous monocot banana like plant that grows 4–8 m in height which grown as a food crop (Minta et al., 2018; Woldesenbet et al., 2020) in the study area.

Table 2. Details of remote sense data for the study.

No.	Sensors ID and types	Acquisition year	Spatial Resolution (m)	Path/row	Sources
1	Landsat 5 TM	1985	30 * 30	169/055	USGS
2	Landsat 7 ETM+	2000	30 * 30	169/055	USGS
3	Landsat 8 OLI-TIRS	2021	30 * 30	169/055	USGS

pixel manner (Teferi et al., 2013). Hence, the supervised classification with a maximum likelihood classifier, which assigns each pixel to the class with the highest probability was used in this study (Degife et al., 2019; Sisay et al., 2021). The LULC classifications from the three Landsat images of the watershed depended on the nature, purposes and resolution of the satellite images (Ewunetu et al., 2021). For example, we classified settlements as farmland determined by the following reasons. Firstly, the year 1985, most dwellings roofs were built from lawns and straws, and they look noticeably like farmland in the images. On other hand, in 2021, most of the dwellings were built from corrugated iron and thus do not have similar reflectance as the 1985 dwelling types as indicted in a previous study (Belay and Mengistu, 2019; Ewunetu et al., 2021; Sisay et al., 2021). Secondly, the watershed is predominantly rural; most dwellings' are scattered and small in size, and they are almost surrounded by farmland. This makes it problematic to identify settlements from farmland at a 30-m resolution in Landsat images.

By comparing the classified maps with reference maps, the accuracy assessment procedures were employed to estimate the accuracy of image classifications. As a result, the Kappa coefficient was used to investigate producer accuracy and overall accuracy as part of the full accuracy assessment (Tewabe and Fentahun, 2020). The entire number of randomly generated error matrix reference values divided by the sum of correctly classified values (diagonals) equals overall accuracy (Lillesand et al., 2004). In comparison to reference data, the Kappa coefficient indicates the difference between actual classified map agreement and chance agreement of random classifier (Minta et al., 2018). Hence, the Kappa coefficient was calculated as follows (Eq. 1):

$$K_{hat} = \frac{N\sum_{i=1}^{r} X_{ii} - \sum_{i=1}^{r}(X_{i+} * X_{+i})}{N^2 - \sum_{i=1}^{r}(X_{i+} * X_{+i})} \quad (1)$$

where; K_{hat} refers to the Kappa coefficient, N refers to the total number of values, $N\sum_{i=1}^{r} X_{ii}$ refers to observed accuracy and $\sum_{i=1}^{r}(X_{i+} * X_{+i})$ refers to chance accuracy.

2.3.1.3. LULC change detection and trend analysis. Change detection is used to determine the extent of changes that occur over time and to categorize changes so that appropriate decisions can be made in various LULC classes (Berihun et al., 2019; Belete et al., 2020). Therefore, LULC change detection analysis throughout three time periods (1985–2000, 2000–2021, and 1985–2021) was done for the study site. The analysis of LULC change detection was compared after classification, as this method is commonly used to compare maps from multiple sources and gives extensive from-to-change class information (Teferi et al., 2013). The outcome of matrix analysis is best expressed by matrix diagram, which generate a theme layer with a different class for each class overlap between two layers. The columns and rows of the matrices are represented by the classes of the two input layers (Hailu et al., 2020). The output of land use classifications was assigned based on how closely whatever two input classes matched. According to Minta et al. (2018), the magnitude of changes among time scales was computed using percent and rate changes of distinct LULC classes. The magnitude of change of each land use type was computed as the following equations (Eqs. (2) and (3)):

$$R\Delta(\%) = \left(\frac{T_2 - T_1}{T_1}\right) * 100 \quad (2)$$

$$Rate\ of\ change\ \left(ha \Big/ year\right) = \left(\frac{T_2 - T_1}{J}\right) \quad (3)$$

where; RΔ (%) represents the change of one type of LULC in percentage between the initial period (T_1) and the subsequent period (T_2) of a LULC class in hectares and J represents the time interval between T_1 and T_2 in a study year.

Furthermore, according to Sisay et al. (2021), the percentages of "conversion loss to" or "conversion gain from" according to Eqs. (4) and (5) relate to the overall loss or gain within every LULC class from 1985 to 2021. In change matrix A, for LULC class i,

$$P_{loss(i),\,j} = \left(P_{i,j} - P_{j,i}\right) / \left(P_{ci} - P_{ri}\right) * 100, \quad i \neq j \quad (4)$$

$$P_{gain(i),\,j} = \left(P_{j,i} - P_{i,j}\right) / \left(P_{ci} - P_{ri}\right) * 100, \quad i \neq j \quad (5)$$

where; $P_{loss(i),\,j}$ is the proportion of the total "conversion loss" of a class row that is taken up by LULC class j *i*; $P_{gain(i),\,j}$ represents the percentages of the entire "conversion gain" of class row i that is acquired by class j; $P_{i,\,j}$ and $P_{j,\,i}$ represent the specific entries in a particular change matrix; P_{ci} is the total of class column *i*; and P_{ri} is the total class of row *i*.

To generate a pair of grid cells that swap any grid cell that gains with a grid cell that loses, the number of swaps of land class (Sj) were computed as two times the minimum of the gain and loss (Yesuph and Dagnew, 2019; Ewunetu et al., 2021). Swap specifies a simultaneous gain and loss of a land-unit type on the landscape and accounts for location change. It was computed as the following mathematical equation (Eq. 6):

$$Sj = 2 * Minimum * \left(P_{gain(i),\,j}\ ,\ P_{loss(i),\,j}\right) \quad (6)$$

The category of exchange, or the percentage of a specific class that transfers while the total land area remains the same, is known as the swap (Sj). The term "swap" refers to the fact that a lack of net change in the watershed does not always imply a lack of LULC change (Yesuph and Dagnew, 2019).

In addition, to analyze LULC trends (scales and directions) by using distributions of LULC data during the study period between 1985 and 2021, the linear regression analysis was carried out using MS-excel software 2016 version and the scatter plot technique. This method is used to predict change itself or project future rates and directions from the current values of LULC classes. It is also clarifying some indication of the potential state of the watershed should observed trends continue in the future. The trend analysis is visualized using a scatter plot. The uphill line of scatter plot indicates an increasing trend while the downhill line of the scatter plot shows a decreasing trend of LULC classes. The scatter plot's direction is calculated using the coefficient of determination, which could be positive or negative (Naikoo et al., 2020).

2.3.1.4. Derivation of agro-ecologies and slope gradients. Agro-ecologies and slope gradients were spawned from DEM (30-m resolution) using Arc GIS10.8. To analyze LULC dynamics and their patterns across agro-ecologies and slope gradients, the three agro-ecologies and six slope categories that consider elevation and slope rolling derived from DEM were delineated and extracted from LULC maps of the three reference study periods (1985, 2000 and 2021) in the watershed. This is necessary for presenting thematic information showing the relationship between variations in each category of land use type within topographic characteristics and agro-ecological zones.

2.3.2. Method of socioeconomic data analysis

Data collected through FGDs (8) and KIIs (45) were identified to rank the major drivers of LULC dynamics in the study area. We obtained population data for the study area from the Central Statistical Agency (CSA) of Ethiopia. Also, data obtained from KIIs were tallied and changed to percentages. Moreover, qualitative data collected from FGDs were analyzed through qualitative methods such as narrations and a thematic analysis approach which similar themes on particular aspects of the studies were grouped and interpreted based on theoretical concepts and underpinning the research objectives. Finally, all results were triangulated with quantitative information such as satellite images.

3. Result and discussion

3.1. Accuracy assessment

The percentages of user and producer accuracies of the classified LULC classes were computed for the three reference years. The classified LULC images for 1985, 2000, and 2021 were created using the supervised Maximum Likelihood technique. The total accuracies of LULC classified images were determined to be 87.55%, 91.14%, and 89.79% in 1985, 2000, and 2021, respectively. The overall Kappa statistics for LULC images from 1985, 2000, and 2021 were found to be 83.72, 88.39, and 86.07, respectively. As a result, the overall accuracies and the Kappa statistics in this study show a strong agreement of classified LULC images for the years 1985, 2000, and 2021, as recommended by Viera and Garrett (2005). This demonstrates that the LULC images were correctly classified in this study.

3.2. Spatio-temporal distributions of LULC

In this section, the distributions of spatio-temporal LULC dynamics were analyzed by using three satellite images and field data between the periods of 1985 and 2021. During these periods, five LULC classes were identified including bareland, farmland, forestland, grassland and shrubland. Analysis of satellite image showed the landscapes was dominantly covered by shrubland (41.87%) and farmland (29.09%) followed by grassland (17.15%), forest (10.19%) and bareland (1.7%) in 1985. In 2000, the proportions of farmland, shrubland and forest area were 51.46%, 23.98% and 11.97%, respectively. The remaining shares of the study area were under bareland (6.59%) and grassland (6%). The dominant land use types in 2021 were under farmland, shrubland and forest which accounted for 71.12%, 12.6% and 7.3%, respectively. The remaining proportions of the watershed were bareland (6.89%) and grassland (2.09%) during the same year.

The trends of LULC changes varied evidently between land use types during three reference study periods. The proportion of bareland increased by 288.5% or 7.8% year^{-1} from 1985 to 2000 and 305.9% or

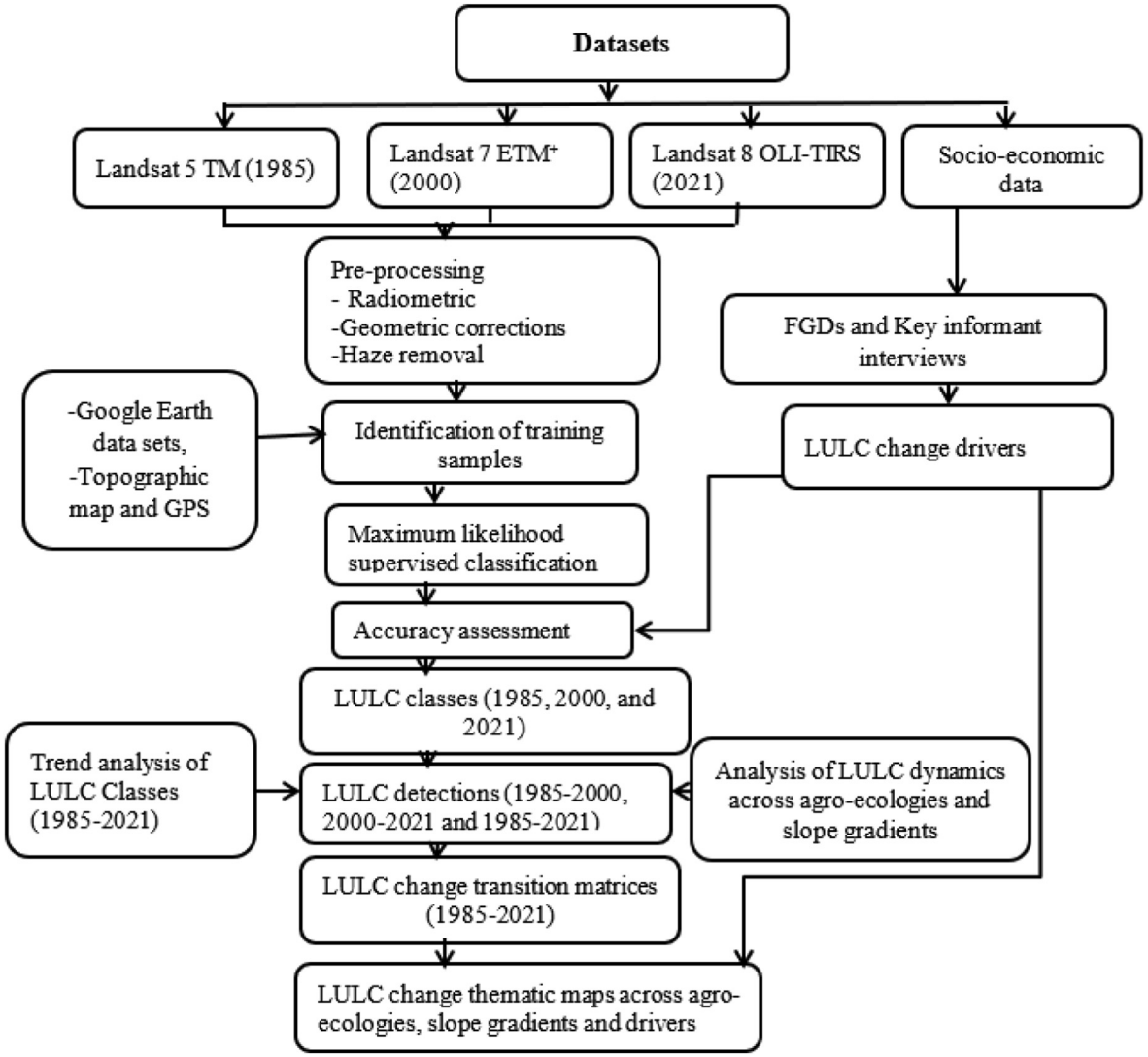

Figure 3. Methodological flowchart of the study.

8.27% year^{-1} from 2000 to 2021 owing to the expansion of marginal area cultivations and overgrazing in the outlet area of the watershed. It was slightly expanded from the northwest to the south part of the watershed. Similarly, farmland showed growing tendencies by 76.89% in 1985–2000 and 144.5% or 3.9% year^{-1} between 2000 to 2021 as rain-fed agriculture is the major source of livelihood (Figure 4 and Table 3). Similar results were reported in various parts of the globe. For instance, agriculture expanded due to increasing demand for food products in Brazil, Africa, Central Asia, Eastern China and Southeast Asia (Hu et al., 2021). Likewise, Potapov et al. (2022) found that the largest net cropland expansion was in Africa, followed by Asia and South America. This expansion is emblematic in Sub-Saharan Africa in general and east Africa in particular due to a growing demand for food is forcing an agricultural rise in formerly less developed savannas and woodlands (Bullock et al., 2021). Also, other recent LULC change studies in different parts of the country witnessed the expansion of farmland to the detriment of shrub-land and forest land (Gashaw et al., 2017; Minta et al., 2018; Belay and Mengistu, 2019; Betru et al., 2019; Degife et al., 2019; Gessesse et al., 2019; Abera et al., 2020; Hailu et al., 2020; Ogato et al., 2021; Sisay et al., 2021). For instance, Gashaw et al. (2017) conducted a study in the Andassa watershed showed the cropland increased from 62.7 to 76.8% during 1985–2015. On the other hand, shrubland, grassland and forest experienced a declining rate during 1985–2021 in the watershed-induced expansion of farmland, deforestation and population growth. During these periods, shrubland, grassland and forest area exhibited a decreasing rate of −1.89%, −2.37% and −0.77% year^{-1}, respectively (Figure 3 and Table 3). However, such trends of these land use types decline is not uniform throughout the country signifying LULC dynamics are site-dependent, socioeconomic and cultural activities (Birhane et al., 2019). In comparison, the reduction was largest for grassland followed by shrubland, this is due to various encroachment of natural associated drivers, human activities and continued increase in livestock. Similarly, the declining tendencies of grassland, forest and shrubland were reported in different parts of Ethiopia: Agidew and Singh (2017) in Teleyayen sub-watershed; Betru et al. (2019) in the Assosa zone; Belay and Mengistu (2019) in Upper Blue Nile basin; Dibaba et al. (2020) in Finchaa Catchment; Tolessa et al. (2020) in Didessa sub-basin and Ogato et al. (2021) in Huluka watershed.

3.3. Spatio-temporal conversions and trajectories of LULC change between 1985 and 2021

In LULC studies, transformations of LULC dynamics from one category to another are quite common (Gashaw et al., 2017). The LULC matrix showed how the extent and direction of LULC categories changed over time. Table 4 and Figure 5 show the results of a conversion matrices' analysis among the LULC classes in the Zoa watershed from 1985 to 2021.

During these periods, significant LULC conversations have been observed with a remarkable LULC conversion index (Table 5 and Figure 5). About 59.71% of the land use types were converted to one of the LULC classes, whereas 40.29% of the LULC categories were left unaltered. Accordingly, the majority of shrubland (1646.35 ha) and forest (784.68 ha) were converted into bareland, while some shares of farmland (738.53 ha) and grassland (588.33 ha) were changed into bareland. Also, a notable amount of shrubland (16,607.43 ha) and grassland (9277.52 ha) were converted into farmland, while some amount of forest (1112.20 ha) and bareland (648.90 ha) during these periods. In line with this study, Hailemariam et al. (2016) found that a large ratio of shrubland was converted into farmland between 1985 and 2016 in the Bale Mountain Eco-Region of Eastern Ethiopia. In comparison to the rest of the LULC classes in the watershed, a large amount of forest area was converted from shrubland (960.08 ha) and grassland (33.75 ha). Whereas, very small proportions of farmland (22.91 ha) and bareland (1.19 ha) were converted into the forest area. An extensive area of grassland was converted from farmland (936.60 ha) and shrubland (192.48 ha), while a very small amount of bareland (5.52 ha) and forest area (2.12 ha) were converted into grassland in the watershed. During 1985–2021, a considerable area of farmland (939.13 ha), forest (909.69 ha) and grassland (356.88 ha) was converted into shrubland, while a very small proportion of bareland (3.66 ha) was converted into shrubland in the watershed. During the transition period between 1985 and 2021,

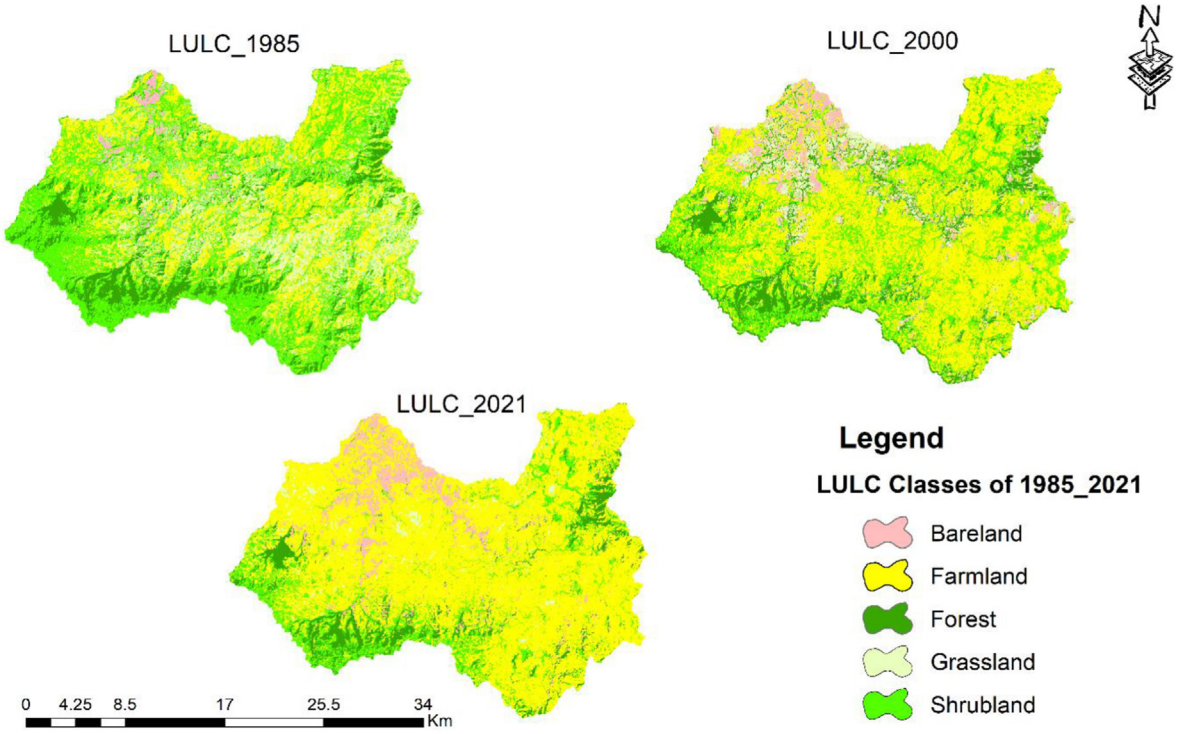

Figure 4. Three reference periods (1985, 2000 and 2021) of LULC maps of the study site.

Table 3. Spatio-temporal distributions of LULC classes in hectares during 1985–2021.

LULC	1985		2000		2021		1985–2000		2000–2021		1985–2021	
	Area (ha)	%	Area (ha)	%	Area (ha)	%	Area (ha)	%	Area (ha)	%	Area (ha)	%
Bareland	1017.1	1.7	3951.27	6.59	4128.69	6.89	2,934.17	288.5	177.42	4.5	3111.59	305.9
Farmland	17425.7	29.09	30823.99	51.46	42604.2	71.12	13398.29	76.89	11780.2	38.2	25178.5	144.5
Forest	6104.03	10.19	7168.34	11.97	4372.21	7.3	1064.31	17.4	−2796.13	−39.0	−1731.82	−28.4
Grassland	10273.16	17.15	3593.93	6.0	1251.38	2.09	−6679.23	−65	−2342.55	65.2	−9021.78	−87.8
Shrubland	25081.8	41.87	14364.26	23.98	7545.32	12.6	−10717.54	−42.73	−6818.94	−47.5	−17536.5	−69.9
Total	**59901.8**	**100**	**59901.8**	**100**	**59901.8**	**100**	-	-	-	-	-	-

Table 4. LULC change transition matrices in hectare between 1985 and 2021 in Zoa watershed.

To	2000	Bareland	Farmland	Forest	Grassland	Shrubland	Grand Total	Loss
From 1985	Bareland	**398.6**	310.93	40.21	216.77	50.53	1,017.04	401.67
	Farmland	1718.09	**12026.86**	255.67	823.32	2604.26	17,428.2	5,401.34
	Forest	34.63	601.28	**3830.58**	623.68	1014.46	6,104.63	2,274.05
	Grassland	664.15	7039.63	275.18	**592.91**	1702.38	10,274.25	9,681.34
	Shrubland	1134.93	10848.67	2762.48	1336.81	**8994.76**	25,077.65	16,082.89
	Grand Total	3950.4	30,827.37	7,164.12	3593.49	14366.39	59,901.77	-
	Gains	3,551.8	18,800.51	3,333.54	3,000.58	8,371.63	-	-
	Swap	2,034.08	10,802.68	4,548.1	6,001.16	16,743.26	-	-
	Net change	3,150.13	13,399.17	1,059.49	−6,680.76	−7,711.26	-	-
	NP	7.9	1.11	0.28	−11.27	−0.86	-	-
To	**2021**	**Bareland**	**Farmland**	**Forest**	**Grassland**	**Shrubland**	**Grand Total**	**Loss**
From 2000	Bareland	**721.52**	3112.46	6.68	99.65	49.38	3989.69	3268.17
	Farmland	894.67	**27856.83**	144.65	1065.62	1162.92	31124.7	3267.86
	Forest	814.28	1495.13	**3356.25**	1.22	994.17	6661.05	3304.8
	Grassland	1408.42	1825.15	291.31	**52.7**	49.7	3627.28	3575.66
	Shrubland	286.25	8313.69	573.14	34.54	**5291.44**	14499.06	9207.62
	Grand Total	4125.14	42603.26	4372.03	1253.73	7547.61	59,901.78	-
	Gains	3,403.62	14,746.43	1015.78	1201.03	2256.17	-	-
	Swap	6,536.34	6,535.72	2,031.56	2,402.06	4,512.34	-	-
	Net change	135.45	11,441.63	−2,559.88	−2,374.63	−6,951.45	-	-
	NP	0.19	0.41	−0.76	−45.06	−1.31	-	-
To	**2021**	**Bareland**	**Farmland**	**Forest**	**Grassland**	**Shrubland**	**Grand Total**	**Loss**
From 1985	Bareland	**367.79**	648.90	1.19	5.52	3.66	1027.06	659.27
	Farmland	738.53	**14957.64**	22.91	936.60	939.13	17594.81	2637.17
	Forest	784.68	1112.20	**3354.96**	2.12	909.69	6163.65	2808.69
	Grassland	588.33	9277.52	33.75	**116.87**	356.88	10373.35	10256.48
	Shrubland	1646.35	16607.43	960.08	192.48	**5336.58**	24742.92	19406.34
	Grand Total	4125.68	42603.69	4372.89	1253.59	7545.94	59901.79	-
	Gains	3,757.89	27,646.05	1,017.93	1,136.72	2,209.36	-	-
	Swap	1,318.54	5,274.34	2,035.86	2,273.44	4,418.72	-	-
	Net change	3098.62	25,008.88	−1,790.76	−9,119.76	−17,196.98	-	-
	NP	8.4	1.67	−0.53	−78.03	−3.2	-	-

Between 1985 and 2021, the bold diagonal elements show the areal extent in hectares of each LULC class that remained constant (persisted). *Net change = Gain – Loss. **NP = net change/diagonals of each class. ***Swap = Minimum value of gain or loss multiplied by two.

extensive areas of shrubland and grassland were converted into farmland with a conversations rate of 448.85 ha (1.05%) and 250.74 ha (0.58%) per annum, respectively as compared with the transformations of further LULC classes. Agriculture expansion mainly happened at the expense of forest, shrubland and grassland, and essentially took place in many world regions, such as Central and Eastern Asia, US, South America, and Central Africa due to increasing demand for food products (Hu et al., 2021). Likewise, the highest agricultural conversion rate occurred in East Africa threatening critical ecosystems and declining biodiversity (Bullock et al., 2021). Only a small share of bareland was converted to forest and shrubland over the study period.

3.3.1. Net change, gains, losses, swap and persistence ratio of LULC

Between 1985 and 2021, the magnitude and direction of LULC dynamics were more imperative. The net change, areas gained, lost, swapped, and persisted between the LULC classes were calculated using the matrices (Table 4). The off-diagonals in the matrices correspond to conversions from one land use class to the other, and the diagonals in Table 4 illustrate LULC classes' persistence (i.e., no change).

The amount of net change revealed that there were transformations among LULC types. As indicated in Table 4, farmland, bareland and forest area have experienced the highest net positive change, followed by bareland and forest area have shown a net positive change within the

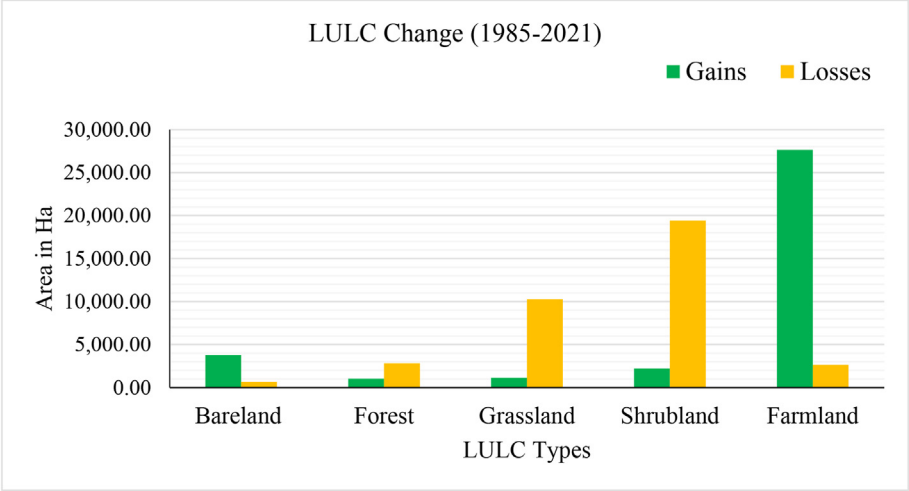

Figure 5. Gains and losses of the LULC classes during 1985–2021.

Table 5. Analysis of LULC dynamics and their patterns across agro-ecologies during 1985–2021.

Years	Agro-ecologies	LULC classes in ha					Total (ha)
		Bareland	Farmland	Forest	Grassland	Shrubland	
1985	Lowland (*Kola*)	901.78	6123.21	606.7	2988.54	6411.65	17031.88
	Midland (*Woina dega*)	115.33	10981.15	4664.64	7101.27	15445.88	38308.27
	Highland (*Dega*)	0	321.36	832.69	183.35	3224.25	4561.65
	Total	1017.1	17425.7	6104.03	10273.16	25081.8	59901.8
2000	Lowland (*Kola*)	3042.76	6949.22	1619.085	2527.74	2895.25	17034.055
	Midland (*Woina dega*)	804.03	22652.99	4396.53	947.78	9502.86	38304.19
	Highland (*Dega*)	104.47	1221.78	1152.73	118.41	1966.15	4563.54
	Total	3951.27	30823.99	7168.34	3593.93	14364.26	59901.8
2021	Lowland (*Kola*)	3120.80	12629.54	80.26	650.14	694.29	17175.03
	Midland (*Woina dega*)	996.45	28634.7	3354.31	596.74	4958.45	38540.65
	Highland (*Dega*)	11.44	1339.97	937.64	4.50	1892.58	4186.13
	Total	4128.69	42604.21	4372.21	1251.38	7545.32	59901.8
1985–2000	Lowland (*Kola*)	+2140.98	+826.01	1012.385	−460.8	−3516.4	-
	Midland (*Woina dega*)	+688.7	+11671.84	−268.11	−6153.49	−5943.02	-
	Highland (*Dega*)	+104.47	+900.42	+320.04	−64.94	−1258.1	-
	Total gain/loss	+2934.17	+13398.29	+1064.31	−6679.23	−10717.54	-
2000–2021	Lowland (*Kola*)	+78.04	+5680.32	−1538.83	−1877.6	−2200.96	-
	Midland (*Woina dega*)	+192.42	+5981.71	−1042.22	−351.04	−4544.41	-
	Highland (*Dega*)	−93.03	+118.19	−215.09	−113.91	−73.57	-
	Total gain/loss	+177.42	+11780.22	−2796.13	−2342.55	−6818.94	-
1985–2021	Lowland (*Kola*)	+2219.02	+6506.33	−526.44	−2338.4	−5717.36	-
	Midland (*Woina dega*)	+881.12	+17653.55	−1310.33	−6504.53	−10487.43	-
	Highland (*Dega*)	+11.44	+1018.61	+104.95	−178.85	−1331.67	-
	Total gain/loss	+3111.59	+25178.51	−1731.82	−9021.78	−17536.48	-

study period of 1985–2000. In contrast, a net negative change in shrubland and grassland was recorded, probably as a result of over-grazing and farming expansions throughout the same study period. During the study period of 1985–2000, the highest loss was occurred in shrubland, followed by grassland, while the highest gain was observed in farmland followed by shrubland and bareland. In addition, the highest net positive change was recorded in farmland followed by bareland within 2000–2021 and 1985–2021 (Table 4). In comparison, the highest net negative change was recorded in shrubland followed by grassland and forest during the same study periods in the watershed. In contrast, the highest gain was observed in farmland, followed by bareland, while the highest loss occurred in shrubland followed by grassland and forest within 2000–2021 and 1985–2021 in the watershed (Table 4 and Figure 5).

Swap is the difference between the total and net change for each category, and it is equivalent to the surface area exchanged across LULC classes (Yesuph and Dagnew, 2019). The highest swap value was experienced in shrubland followed by farmland during 1985–2000, this implies an extensive exchange with other LULC classes, it simultaneously loses and gains surface area from other classes. In comparison, the highest swap value was observed in bareland followed by farmland during 2000–2021. Overall, the highest swap value was recorded in farmland followed by shrubland and grassland, exhibited these LULC classes were the utmost dynamic class in the watershed between 1985 and 2021 (Table 4).

As indicated in Table 4 and Figure 6, regarding the net change-to-persistence ratio to diagonals of each LULC class, grassland (−11.27) had shown the highest net change-to-persistence ratio, followed by

bareland (7.9) and farmland (1.11), while the lowest net change-to-persistence ratio was recorded in shrubland (−0.86), followed by forest (0.28) between 1985 and 2000. On the other hand, the net change-to-persistency ratio was quite high for grassland (45.06), shrubland (−1.31) and forest (−0.76) as contrasted with farmland (0.41) and bareland (0.19) within the study period of 2000–2021. Overall, grassland (−78.03), bareland (8.4) and shrubland (−3.2) had a large net change-to-persistence ratio as contrasted with farmland (1.67) and forest (−0.53). The least persistent LULC class has the highest net change-to-persistence ratio (both negative and positive), while the LULC class with the lowest net change-to-persistence ratio has increased or declined at a faster rate (Dibaba et al., 2020; Sisay et al., 2021).

3.4. Trends of LULC classes between 1985 and 2021

This section presents LULC trends (scales and directions) using distributions of LULC data in Zoa watershed during the study period between 1985 and 2021. A regression analysis model was used since it has a very flexible design and can be used with data that is not evenly spaced over time. It also indicates that LULC classes are unceasingly shaped during the study period with minor and major conversations from one class to the other. As presented in Figure 7, the scatter plots of bareland and farmland show an increasing trend over time and are steady data series revealing dynamics in socio-economic activities at priorities on the rate of overwhelming areas under shrubland, forest and grassland during the study period. Whereas the analysis of scatter plots revealed that forest area, grassland and shrubland exhibit a falling tendency between 1985 and 2021. The regression analysis indicates the land use classes of bareland ($R^2 = 0.70$) and farmland ($R^2 = 0.99$) have a significant positive or direct relationship, while shrubland ($R^2 = 0.95$), grassland ($R^2 = 0.87$) and forest area ($R^2 = 0.47$) have a significant negative or inverse relationship between 1985 and 2021 in the study area. In contrast, the coefficients of the regression showed that the LULC classes of the forest, grassland and shrubland are significantly affected throughout the study period. These are might have an upward trend of farmland and bareland with associated drivers of land use land cover dynamics in the study area.

3.5. LULC dynamics and their patterns across agro-ecologies

Analysis of LULC dynamics and their patterns across agro-ecologies have important implications for sustainable natural resource management decisions since the diverse agro-ecologies and topography need a special management plans. The findings realized that between 1985 and 2021, a significant portion of the landscapes in each of the agro-ecologies practiced various LULC dynamics and trends. During 1985–2021, a large proportion of the bareland was found lowland or *kolla* agro-ecology, while a large proportion of farmland, forest and shrubland were found in midland (*Woina dega*) agro-ecology in the watershed (Table 5 and Figure 8). This is due to the midland sharing a large proportion of the total area of the watershed and it is suitable for human settlements. However, a large part of the grassland was located midland in 1985 and in lowland in 2000 and 2021.

Between 1985 and 2021, the proportion of farmland in all agro-ecologies showed an increasing tendency with the highest rate in the watershed (Table 5 and Figure 8). Likewise, bareland was expanded in all agro-ecologies except in highland during 2000–2021, which might be related to reafforestation programs introduced in the highland areas of the watershed. In contrast, forest area was increased in highland agro-ecologies during 2000–1985 due to Eucalyptus plantations, while it was reduced in lowland and midland agro-ecologies between 1985 and 2021. Over the entire period (1985–2021), grassland and shrubland showed an astonishing decline due to expansion of farmland in adjoining their areas in all agro-ecologies in the watershed. This study consistent with Birhane et al. (2019) and in their study conducted in Northern Ethiopia reported that the reduced amount of these land use types might be due to socioeconomic activities such as cultivations of marginal lands, mainly introduction of sawmills, civil war and cutting shrubs for firewood both for the market and home consumption.

3.6. LULC dynamics in slope gradients

Analysis of LULC dynamics in slope gradients have been imperative due to the ceaseless demand for farmland which brought LULC changes in steep slope gradients. During 1985, a large share of the farmland, grassland and bareland were located in moderate (15–30%) and sloping (5–10%) gradients. Over the same study period, however, a significant amount of the forest area was found in moderately (15–30%) and steeply (30–60%) slope gradients. Furthermore, a high amount of shrubland was located on a moderately slope (15–30%), followed by a strongly slope (10–15%) in the watershed.

In the year 2000, a large proportion of bareland, grassland and shrubland in the watershed was on a moderately rolling slope (15–30%), followed by slope rolling (5–10%). Likewise, a major part of the farmland was experienced in a moderately rolling slope (15–30%) in the watershed. However, a significant portion of forest area was situated in moderate (15–30%) and steep (30–60%) slope gradients (Table 6). A previous

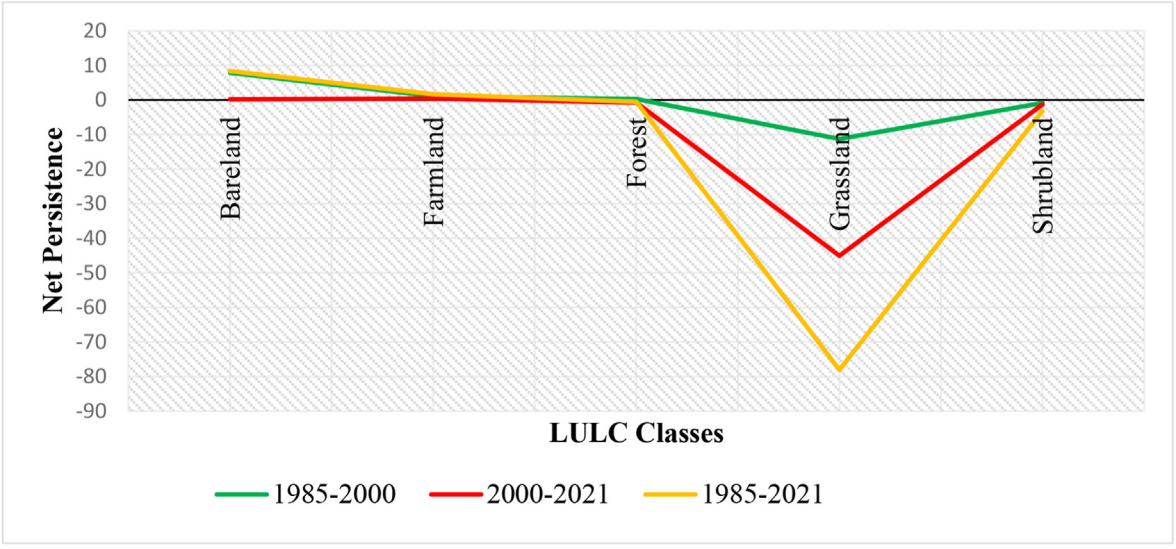

Figure 6. Net change-to-persistence ratio of the LULC classes between 1985 and 2021.

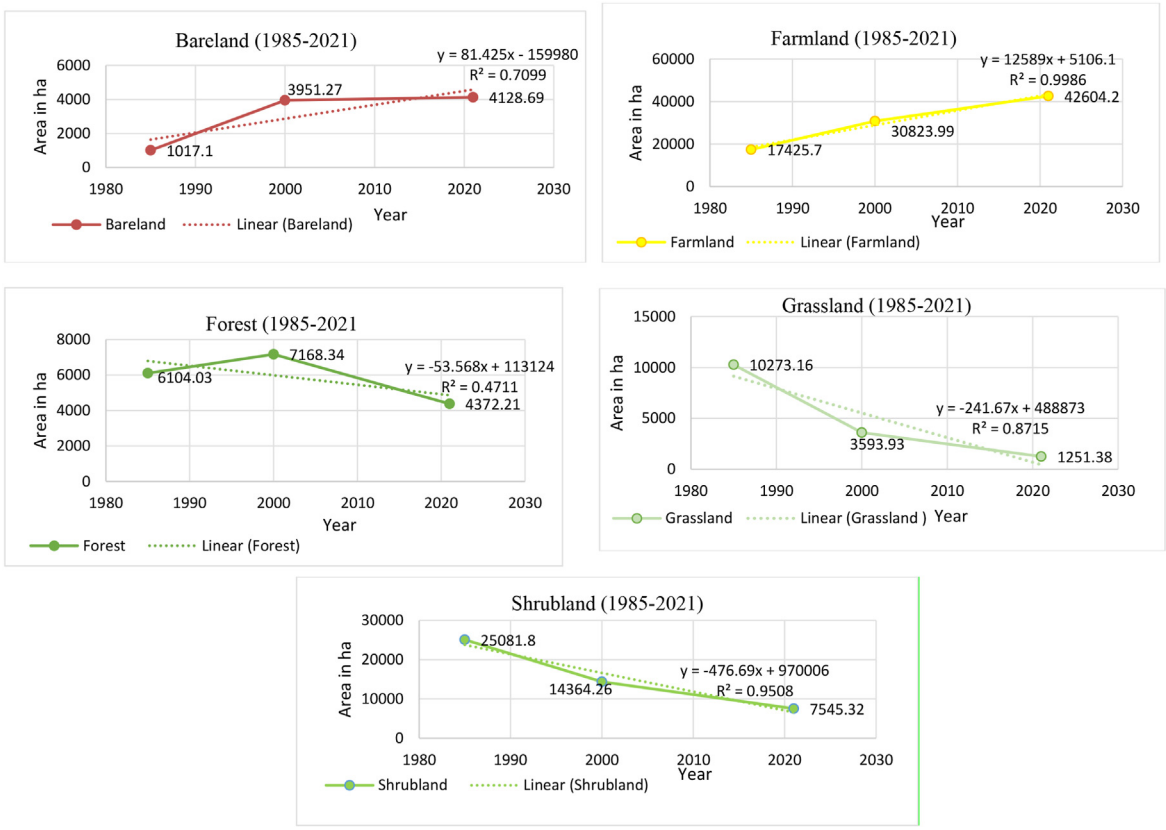

Figure 7. Trend analysis of LULC Classes in the Zoa watershed from 1985 to 2021.

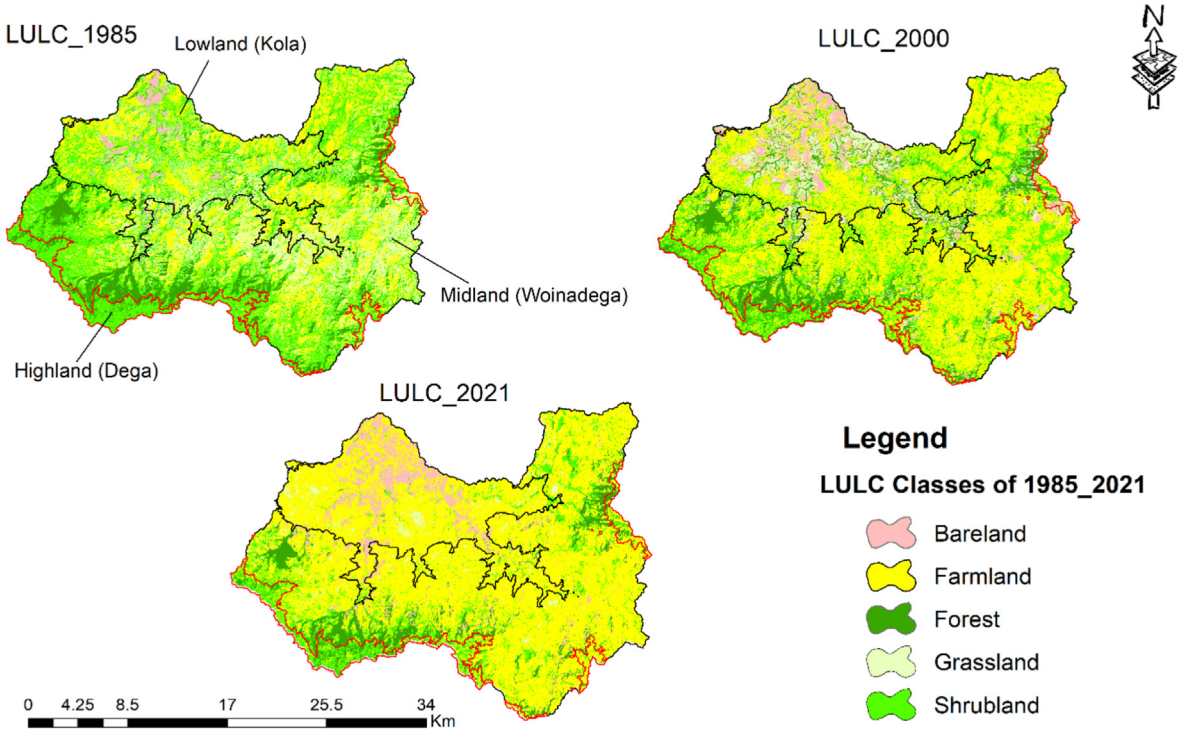

Figure 8. LULC maps across agro-ecologies.

study has validated forest ratio was increased in steep slopes. In line with this study, the increment of forests is more in steep slopes which can be due to the fact that these areas are inaccessible to human activities unlike the moderate and gentle slopes (Birhane et al., 2019). A considerable portion of bareland was placed in moderate (15–30%) and sloping (5–10%) slope gradients in 2021, whilst forest area was situated in

Table 6. Analysis of LULC dynamics in slope gradient during 1985–2021.

Years	LULC types	Slope classes in percent rise and area coverage in ha						
		0–5%	5–10%	10–15%	15–30%	30–60%	>60%	Total
1985	Bareland	126.59	282.88	205.17	349.52	52.97	0	1017.13
	Farmland	1720	4336.6	3648	6544.65	1173.62	2.83	17425.7
	Forest	133.87	450.15	616.3	2686.3	2199.41	18	6104.03
	Grassland	757.58	2180.35	2088.3	4303.13	941.63	2.178	10273.168
	Shrubland	1921.87	5149.9	4747.16	10339.44	2913.18	10.25	25081.8
2000	Bareland	524.86	1077.56	762.84	1236.84	348.24	0.93	3951.27
	Farmland	2548.02	6957.77	6245.44	12420.55	2648.98	3.23	30823.99
	Forest	295.65	841.99	948.92	3094	1973.35	14.43	7168.34
	Grassland	267.86	676.12	568.3	1417.86	654.94	8.85	3593.93
	Shrubland	1005.09	2816.18	2735.64	6126.83	1674.4	6.12	14364.26
2021	Bareland	308.03	758.9	678.2	1692.85	689.48	1.23	4128.69
	Farmland	3559	9578.16	8452.97	17153.04	3852.76	8.27	42604.2
	Forest	103.64	344.1	446.65	1898.99	1562.11	16.72	4372.21
	Grassland	200.13	390.73	256.53	351.37	52.62	0	1251.38
	Shrubland	439.21	1295.5	1363.72	3304.17	1135.84	6.88	7545.32

Note: Flat = 0–5; sloping = 5–10; strongly sloping = 10–15; moderately sloping = 15–30; steep = 30–60; very steep=>60.

moderate (15–30%) and steep (30–60%) slope gradients. A lion share of farmland was found in moderate (15–30%) slope gradient, followed by sloping gradient (5–10%) in the watershed. In the watershed, a significant amount of shrubland was identified with a moderate (15–30%) and strong (10–15%) slope gradient.

In contrast, farmland was increased on moderately and steeply rolling slopes. This is due to rapid human population growth and continued demand for agriculture. For instance, farmland was identified over a steep slope 1173.62 ha in 1985, 2648.98 ha in 2000 and 3852.76 in 2021. Likewise, Kindu et al. (2013) reported the expansion of cultivated land from gentle and moderate slopes to steep and very steep slopes of the Ethiopian highlands. The increment of the farmland might be related to accessibility and suitability of land. This condition exacerbates soil erosion in undulating topography which in turn leads to bareland unless adequate conservation measures are taken. Similarly, bareland showed a growing trend toward moderate to steep slope gradients, possibly due to pressures on forest and shrubland, such as overgrazing in rough terrain.

4. Major drivers of LULC dynamics in the study area

LULC changes are a direct outcome of both human and natural factors, with anthropogenic pressure owing to globalization as the foremost driver (Regasa et al., 2021). Such an opinion concerning various parts of Ethiopia is also presented by other authors, emphasizing the common and simultaneous effect of the interaction of natural and anthropogenic driving factors (Betru et al., 2019; Degife et al., 2019; Aneseyee et al., 2020; Dibaba et al., 2020; Sisay et al., 2021). However, human activities were found to be main and abrupt as compared to the natural process as a driver of LULC dynamics (Dibaba et al., 2020). Some drivers are well related to the results and analysis of Landsat images. However, the major drivers are not only restricted in the watershed, rather they are also issued of different parts of Ethiopia. Because of that, the key informants identified the following proximate (direct) and underlying (indirect) drivers in the watershed.

4.1. Proximate drivers

According to data gathered from key informants, six major proximate drivers of LULC dynamics were identified in the watershed. The majority of interviewees (95.6%) perceived that the expansion of farmland and settlement was the foremost proximate driver of LULC dynamics (Figure 9). This is supported by the LULC analysis which showed the increasing tendency of the farmland class from 29.09% in 1985 to 51.46% in 2000 to 71.12% in 2021. Besides, the summary of the focus group discussions revealed that the unintended expansion of farmland and settlement on the way to the surrounding shrubland and forest area is the main driver of the LULC dynamics in the watershed. In line with this, similar results were reported in different parts of Ethiopia (Berihun et al., 2019; Betru et al., 2019; Degife et al., 2019; Dibaba et al., 2020; Hishe et al., 2020). For instance, Degife et al. (2019) asserted that the expansion of cropland exerts puts a lot of pressure on the natural resources in Lake Hawassa watershed of Ethiopia.

About 86.7% of interviewees asserted extraction of wood for firewood and income sources are also one of the vital drivers contributing to change in LULC in the watershed. Focus group discussants also affirmed that almost all people in the watershed exclusively depend on trees as a source of fuel-wood without replacing for future use. This is because of the absence of additional power such as electric, solar and extra renewable energy sources. Moreover, key informants from the upper watershed also attested that most residents are using trees as a main source of revenue due to the increasing demand for extraction of charcoal, firewood sale, local furniture and construction purposes without reforestation. Similarly, Hishe et al. (2020) reported that one more serious issue is the extraction of trees/wood for domestic and commercial purposes, which is primarily done by residents and or sometimes by illegal traders.

LULC dynamics in the watershed, according to 71.1% of interviewees, are driven by uncontrolled grazing. Besides, the results indicated by focus group participants in the lower streams confirmed that climate variability and overgrazing created high pressure on grassland and bushland which in turn the grassland might be converted into bareland through time, and thereby rising soil erosion around the outlet area. This finding corroborates LULC analysis which revealed that grassland and bushland have exhibited a declining tendency since 1985. Likewise, due to climate change and human activity effects, grassland ecosystems are being invaded by other land use types in many regions of the world (Shen et al., 2022b; Xu et al., 2022). Similarly, prior studies reported that uncontrolled grazing of animals, hampered forest succession by destroying emerging seedlings and browsing, particularly of olive trees in the country (Hishe et al., 2020).

It is indicated in Figure 9, about 73.3% of interviewees maintained that terrain features (slope and aspects) were further drivers of LULC dynamics in the watershed. Similar findings were reported in different parts of Ethiopia (Kindu et al., 2015; Yesuph and Dagnew, 2019; Ogato et al., 2021).

Predominated share of (71.1%) of interviewees declared that forest fire was the noticeable driver of LULC dynamics. Hence, it needs an

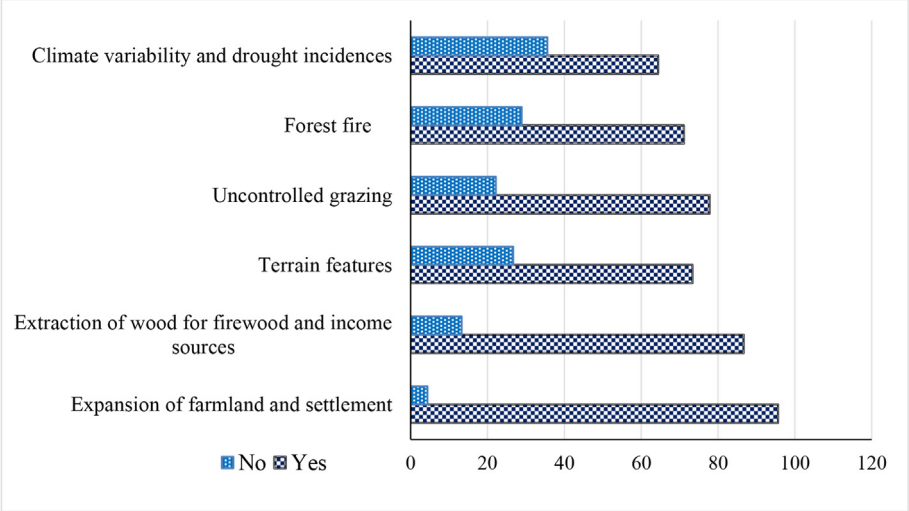

Figure 9. Proximate major drivers of LULC perceived by interviewees. Note: Multiple responses were provided.

urgent response; if not, it will result in environmental degradation, especially, in the bottom and outlet parts of the watershed. Moreover, about 64.4% of the interviewees specified that drought incidences including erratic rainfall were considered the drivers of LULC change. According to Gitima et al. (2021), both minimum and maximum temperature were increased with the seasonal erratic nature of rainfall bringing indescribable hardship in the Dawuro zone. In addition, focus group discussants recognized that the increasing trends of temperature and shifting of seasonal weather phenomenon cause LULC dynamics. Belay and Mengistu (2019) also confirmed that climate variability and change could lead to land conversion for various purposes.

4.2. Underlying drivers

Rapid human population growth in the study area was specified by interviewees (91.1%) as one of the utmost important underlying drivers of LULC dynamics. It was understood by focus group discussants that the population is growing alarmingly in the watershed due to natural increases; this exacerbates the expansion of farmland towards shrubland and forest without concerning regional land use planning with natural resource management. This is in line with total population data from 1984 to 2021 of the study area (CSA, 2022) and the average growth rate of 278.28 or 7.3 by annually (Figure 10). The expansion of farmland during the study period was consistently associated with this population growth in a positive way. Rapid human population growth is confirmed as a major driver of LULC dynamics in different parts of Ethiopia (Abebe et al., 2019; Berihun et al., 2019; Betru et al., 2019; Abera et al., 2020; Hailu et al., 2020; Ogato et al., 2021; Sisay et al., 2021). For instance, Hailu et al. (2020), both forest cover and wetland proportions encroachment, new farmland, and firewood extraction resulted from the rapid growth of human population and demand for cultivated land, biofuels and construction. Moreover, Abera et al., 2020) affirmed that population density and rapid population growth exacerbate the rate of resource depletion in the Chewaka district of Ethiopia. Regasa et al. (2021) based on the a literature review underlined unfavorable changes in LULC as a consequence of increasing human pressure on the Ethiopian environment driven by the need of improving the socioeconomic situation of the local population.

The poor land tenure system including policy is also affirmed by interviewees (68.9%) as an important driver for the LULC dynamics (Figure 11). Focus group discussants asserted that the land tenure policy system in the country discourages rural land ownership rights, this could be related to a decrease in resource conservation and an upsurge in deforestation and forest degradation. Likewise, Sisay et al. (2021) reported that land policies with poor regulations are derived from each regime's political ideologies in Ethiopia, land policies change with each change of government. The land tenure policy was changed from private ownership to state and private (feudal) ownership when the Derg regime abandoned the imperial government in 1974. Moreover, Tefera (2011) and Hailu et al. (2020) reported that due to a change in land policy under the regime of Derge, extensive portions of forest and pasture land were transformed for various land uses. These poor land tenure policies contributed significantly to the fast transformation of rural land from one land use type to another under each regime.

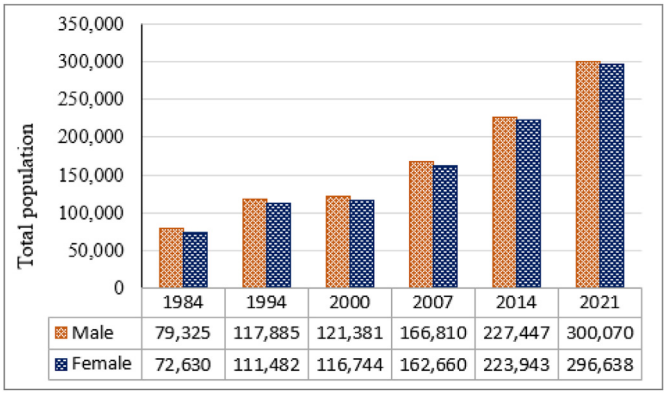

	1984	1994	2000	2007	2014	2021
Male	79,325	117,885	121,381	166,810	227,447	300,070
Female	72,630	111,482	116,744	162,660	223,943	296,638

Figure 10. The total number of population (1984–2021) in the watershed (CSA, 2022).

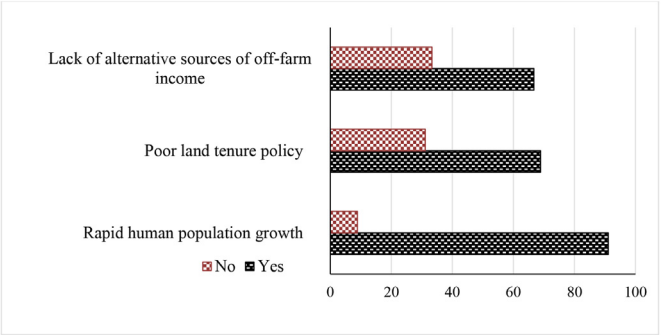

Figure 11. Underlying major drivers of LULC perceived by interviewees. Note: Multiple responses were provided.

Another driver of LULC dynamics identified by interviewees (66.7%) in the watershed is a lack of off-farm activities (Figure 11). Besides, focus group discussants also confirmed that the majority of the rural communities in the watershed are relying on rain-fed agriculture. In the watershed, there was no off-farm diversification other than selling firewood and charcoal, which accelerated deforestation and LULC changes. Belay and Mengistu (2019) stated that youthful and landless peasants, who make a living by producing charcoal and cutting trees for cultivating land, were among the main causes of forest resource decrease. Hence, with assistance and support in the form of capacity building, they are being encouraged to diversify off-farm income-generating enterprises, provision of credit and facilitating markets (Agidew and Singh, 2017) are recommended to address these problems in the watershed.

5. Conclusion

The diverse agro-ecology and slope gradient in Ethiopia necessitates site-specific LULC studies at a watershed level. This study is, therefore, intended to examine the spatio-temporal LULC dynamics across agro-ecologies and slope gradients using geospatial technologies in Zoa watershed of Omo-Gibe basin over the period of 1985–2021. Unfortunately, the changes found should be considered unfavorable and may lead to environmental degradation by strengthening and intensifying the phenomenon of erosion or loss of soil organic matter. The reason for such a situation was the fact that an extensive area of shrubland and grassland were converted into farmland. This was expanded towards moderately and steep rolling slopes from 1985 to 2021. Additionally, the coefficients of the model of regression reveal that the LULC classes of the forest, grassland and shrubland are significantly affected throughout the study period. It was found that between 1985 and 2021, the proportion of farmland in all agro-ecological zones showed an increasing tendency with the highest rate in the watershed. In contrast, forest area was increased in highland agro-ecological zones during 2000–1985 due to the launch of new plantation sites, while it was decreased in lowland and midland agro-ecological zones between 1985 and 2021. Farmland was expanded towards moderately and steep rolling slopes due to population growth and ongoing demand for agricultural land. This is due to Ethiopia has not a clear land use policy that prohibits the use of steep slope areas for agriculture. This condition exacerbates soil erosion in undulating topography unless adequate conservation measures are taken through land use policy interventions in the country. The foremost direct and indirect drivers of LULC dynamics are found to be an expansion of farmland and settlement and rapid human population growth, respectively. The overall result confirmed that farmland and barelands are expanding at the expense of other land use types. This might lead to serious environmental problems like climate change, soil erosion and biodiversity loss. Thus, the confined government in consultation with the community and other stakeholders should work on redesigning effective management strategies through appropriate land use planning to address the adverse effects of LULC dynamics.

It is well known that any LULC map derived from satellite images has errors or uncertainties (Hu et al., 2020; Hussain et al., 2022; Shen et al., 2022a). Limitations of the satellite data resolutions, imperfect adjustment data, and empirical model precision are the primary causes of image class omission and commission errors. Landsat clear-sky data availability is the key limitation for land cover mapping. To reduce this uncertainty, we obtained remotely sensed data in dry season of Ethiopia. This technique is very efficient at minimizing cloud cover, various other noise issues, and eliminates temporal data (Shen et al., 2022a). While some of the land cover themes can be directly mapped using a single-day satellite images, others may not be directly retrieved from the optical medium resolution data. The incompleteness of the Landsat observation time series decreases map accuracy in a given area with persistent cloud cover (Potapov et al., 2022). Moreover, pixels are acquired at different times and different viewing geometries, under different atmospheric conditions (Shen et al., 2022a).

Declarations

Author contribution statement

Ginjo Gitima: Conceived and designed the experiments; Performed the experiments; Analyzed and interpreted the data; Wrote the paper.

Menberu Teshome, Meseret Kassie and Monika Jakubus: Conceived and designed the experiments; Analyzed and interpreted the data; Contributed reagents, materials, analysis tools or data; Wrote the paper.

Funding statement

This research did not receive any specific grant from funding agencies in the public, commercial, or not-for-profit sectors.

Data availability statement

Data associated with this study has been deposited at http://earthexplorer.usgs.gov

Declaration of interest's statement

The authors declare no conflict of interest.

Additional information

No additional information is available for this paper.

Acknowledgements

We would like to thank Bonga University and University of Gondar for their support to the corresponding author who is a Ph.D. candidate. We thank also the Ethiopian Geospatial Information Agency (EGIA) for providing important geospatial data for this study. Our heartfelt thanks go to the residents of the Zoa watershed and stakeholders for their sharing vital data and experiences.

References

Abdo, Z.A., Prakash, S., 2020. A review paper on monitoring environmental consequences of land cover dynamics with the help of geo-informatics technologies. Geosfera Indon. 5 (3), 364–377.

Abebe, M.S., Derebew, K.T., Gemeda, D.O., 2019. Exploiting Temporal - Spatial Patterns of Informal Settlements Using GIS and Remote Sensing Technique : a Case Study of Jimma City , Southwestern Ethiopia. Environmental Systems Research [Preprint].

Abera, A., Yirgu, T., Uncha, A., 2020. Impact of Resettlement Scheme on Vegetation Cover and its Implications on Conservation in Chewaka District of Ethiopia. *Environmental Systems Research* [Preprint].

Agidew, A., Singh, K.N., 2017. The Implications of Land Use and Land Cover Changes for Rural Household Food Insecurity in the Northeastern highlands of Ethiopia : the Case of the Teleyayen Sub - Watershed. Agriculture & Food Security, pp. 1–14.

Aneseyee, A.B., Soromessa, T., Elias, E., 2020. The effect of land use/land cover changes on ecosystem services valuation of Winike watershed, Omo Gibe basin, Ethiopia. Human Ecol. Risk Assess. 26 (10), 2608–2627.

Auch, R.F., Wellington, D.F., Taylor, J.L., Stehman, S.V., Tollerud, H.J., Brown, J.F., et al., 2022. Conterminous United States land-cover change (1985–2016): new insights from annual time series. Land 11 (2), 298.

Bantider, A., Hurni, H., Zeleke, G., 2011. Norsk geografisk tidsskrift - responses of rural households to the impacts of population and land-use changes along the eastern escarpment of wello , Ethiopia. Norsk Geografisk Tidsskrift - Norwegian J. Geog. 65 (1), 42–53.

Belay, T., Mengistu, D.A., 2019. Remote sensing applications : society and environment land use and land cover dynamics and drivers in the muga watershed , upper blue Nile basin , Ethiopia. Remote Sens. Appl.: Society and Environ. 15, 100249.

Belete, M., Deng, J., Abubakar, G.A., Teshome, M., Wang, K., Woldetsadik, M., et al., 2020. Partitioning the impacts of land use/land cover change and climate variability on water supply over the source region of the Blue Nile Basin. Land Degrad. Dev. 31 (15), 2168–2184.

Berihun, M.L., Tsunekawa, A., Haregeweyn, N., Meshesha, D.T., Adgo, E., Tsubo, M., et al., 2019. Exploring land use/land cover changes, drivers and their implications in contrasting agro-ecological environments of Ethiopia. Land Use Pol. 87 (March), 104052.

Betru, T., Tolera, M., Sahle, K., Kassa, H., 2019. Trends and drivers of land use/land cover change in Western Ethiopia. Appl. Geogr. 104, 83–93.

Birhane, E., Ashfare, H., Fenta, A.A., Hishe, H., Gebremedhin, M.A., Solomon, N., 2019. Land use land cover changes along topographic gradients in Hugumburda national forest priority area, Northern Ethiopia. Remote Sens. Appl.: Society and Environment 13, 61–68.

Bullock, E.L., Healey, S.P., Yang, Z., Oduor, P., Gorelick, N., Omondi, S., et al., 2021. Three decades of land cover change in East Africa. Land 10 (2), 150.

CSA, 2022. Dataset Records for Central Statistics Agency of Ethiopia. Accessed in June 23/2022). https://ghdx.healthdata.org/organizations/central-statistics-agency-ethiopia.

Degife, A., Worku, H., Gizaw, S., Legesse, A., 2019. Land use land cover dynamics, its drivers and environmental implications in Lake Hawassa Watershed of Ethiopia. Remote Sens. Appl.: Soc. Environ. 14, 178–190.

Dibaba, W.T., Demissie, T.A., Miegel, K., 2020. Drivers and implications of land use/land cover dynamics in Finchaa Catchment, Northwestern Ethiopia. Land 9 (4), 1–20.

Eva, H.D., Brink, A.B., Simonetti, D., 2006. Monitoring Land Cover Dynamics in Sub-saharan Africa. Office for Official Publication of the European Communities, Luxembourg. EUR 22498 EN.

Ewunetu, A., Simane, B., Teferi, E., Zaitchik, B.F., 2021. Land cover change in the blue nile river headwaters: farmers' perceptions, pressures, and satellite-based mapping. Land 10 (1), 68.

FAO, 2006. Guidelines for Soil Description, fourth ed. FAO, Rome, Italy.

Gashaw, T., Tulu, T., Argaw, M., Worqlul, A.W., 2017. Evaluation and prediction of land use/land cover changes in the Andassa watershed, Blue Nile Basin, Ethiopia. Environmen. Sys. Res. 6 (1), 1–15.

Gashaw, T., Tulu, T., Argaw, M., Worqlul, A.W., 2018. Modeling the hydrological impacts of land use/land cover changes in the Andassa watershed, Blue Nile Basin, Ethiopia. Sci. Total Environ. 619, 1394–1408.

Gebrelibanos, T., Assen, M., 2015. Land use/land cover dynamics and their driving forces in the Hirmi watershed and its adjacent agro-ecosystem, highlands of Northern Ethiopia. J. Land Use Sci. 10 (1), 81–94.

Gessesse, A.A., Melesse, A.M., Abiy, A.Z., 2019. Land use dynamics and base and peak flow responses in the Choke mountain range, Upper Blue Nile Basin, Ethiopia. Int. J. River Basin Manag. 19 (1), 109–121.

Gezmu, G.G., Isoda, H., Rahut, D.B., Amekawa, Y., Nomura, H., 2021. Gender differences in agricultural productivity: Evidence from maize farm households in southern Ethiopia. Geo J. 86 (2).

Gitima, G., Legesse, A., 2019. Determinants of farmers' decision to use improved land management practice in gindara watershed, southern Ethiopia. Ethiopian J. Environ. Develop. 2 (2), 17–34.

Gitima, G., Legesse, A., Biru, D., 2021. Assessing the impacts of climate variability on rural households in agricultural land through the application of livelihood vulnerability index. Geosfera Indonesia 6 (1), 96–126.

Habte, D.G., Belliethathan, S., Ayenew, T., 2021. Evaluation of the status of land use/land cover change using remote sensing and GIS in Jewha Watershed, Northeastern Ethiopia. SN Appl. Sci. 3 (4), 1–10.

Hailemariam, S.N., Soromessa, T., Teketay, D., 2016. Land use and land cover change in the bale mountain eco-region of Ethiopia during 1985 to 2015. Land 5 (4), 41.

Hailu, A., Mammo, S., Kidane, M., 2020. Dynamics of land use , land cover change trend and its drivers in Jimma Geneti District , Western Ethiopia. Land Use Pol. 99 (June), 105011.

Haregeweyn, N., Tsunekawa, A., Nyssen, J., Poesen, J., Tsubo, M., Tsegaye Meshesha, D., et al., 2015. Soil erosion and conservation in Ethiopia: a review. Prog. Phys. Geogr. 39 (6), 750–774.

Hishe, H., Giday, K., Haile, M., 2015. The influence of physical factors on deforestation of key species and their implication for forest management in the dry afromontane forest of Desa ' a , northern Ethiopia. Int. J. Sci. Res. 4 (3), 2400–2407.

Hishe, S., Bewket, W., Nyssen, J., Lyimo, J., 2020. Analysing past land use land cover change and CA-Markov-based future modelling in the Middle Suluh Valley, Northern Ethiopia. Geocarto Int. 35 (3), 225–255.

Hu, X., Næss, J.S., Iordan, C.M., Huang, B., Zhao, W., Cherubini, F., 2021. Recent global land cover dynamics and implications for soil erosion and carbon losses from deforestation. Anthropocene 34, 100291.

Hussain, S., Lu, L., Mubeen, M., Nasim, W., Karuppannan, S., Fahad, S., et al., 2022. Spatiotemporal variation in land use land cover in the response to local climate change using multispectral remote sensing data. Land 11 (5), 595.

Jacob, M., Frankl, A., Beeckman, H., Mesfin, G., Hendrickx, M., Guyassa, E., Nyssen, J., 2015. North Ethiopian afro-alpine tree line dynamics and forest-cover change since the early 20th century. Land Degrad. Dev. 26 (7), 654–664.

Jansen, L.J.M., 2010. Analysis of Land Change with Parameterised Multi-Level Class Sets. Ph.D. Thesis. Wageningen University, Wageningen, The Netherlands, p. 7. With summaries in English and Dutch.

Kidane, M., Bezie, A., Kesete, N., Tolessa, T., 2019. The impact of land use and land cover (LULC) dynamics on soil erosion and sediment yield in Ethiopia. Heliyon 5 (12), e02981.

Kindu, M., Schneider, T., Teketay, D., Knoke, T., 2013. Land use/land cover change analysis using object-based classification approach in Munessa-Shashemene landscape of the Ethiopian highlands. Rem. Sens. 5 (5), 2411–2435.

Kindu, M., Schneider, T., Teketay, D., Knoke, T., 2015. Drivers of land use/land cover changes in Munessa-Shashemene landscape of the south-central highlands of Ethiopia. Environ. Monit. Assess. 187 (7), 1–17.

Lambin, E.F., Geist, H.J., Lepers, E., 2003. D ynamics of L and -U Se and L and -C over C hange in T ropical R egions. Annu. Rev. Environ. Resour. 28, 205–241.

Lillesand, T.M., Kiefer, R.W., Chipman, J.W., 2004. Remote Sensing and Image Interpretation, fifth ed. John Wiley & Sons, Hoboken, New Jersey.

Marczyk, G., DeMatteo, D., Festinger, D., 2005. Essentials of Research Design and Methodology. John Wiley & Sons, Hoboken, NJ, USA.

MEA, 2003. 'Ecosystems and Human Well-Being: A Framework for Assessment'. Synthesis. Island Press, Washington, DC.

Minta, M., Kibret, K., Thorne, P., Nigussie, T., Nigatu, L., 2018. Land use and land cover dynamics in Dendi-Jeldu hilly-mountainous areas in the central Ethiopian highlands. Geoderma 314, 27–36.

MOA (Ministry of Agriculture), 1998. Agro ecological zones of Ethiopia, MOA. Addis Ababa, Ethiopia.

Naikoo, M.W., Rihan, M., Ishtiaque, M., 2020. Analyses of land use land cover (LULC) change and built-up expansion in the suburb of a metropolitan city : spatio-temporal analysis of Delhi NCR using landsat datasets. J. Urban Manag. 9 (3), 347–359.

Nigussie, Z., Tsunekawa, A., Haregeweyn, N., Adgo, E., Nohmi, M., Tsubo, M., et al., 2016. Factors affecting small-scale farmers' land allocation and tree density decisions in an acacia decurrens-based taungya system in Fagita Lekoma District, North-Western Ethiopia. Small-Scale Fores. 16 (2), 219–233.

Nkonya, E., Karsenty, A., Msangi, S., Souza Jr., C., Shah, M., Von Braun, J., Park, S., 2012. Sustainable Land Use for the 21st century.

Nkonya, E., Mirzabaev, A., von Braun, J., 2016. Economics of Land Degradation and Improvement—A Global Assessment for Sustainable Development. Springer, Bonn, Germany, pp. 1–14.

Ogato, G.S., Bantider, A., Geneletti, D., 2021. Dynamics of land use and land cover changes in Huluka watershed of Oromia Regional State, Ethiopia. Environ. Sys. Res. 10 (1).

Omran, E.E., 2012. Detection of Land-Use and Surface Temperature Change at Different Resolutions. Journal of Geographic Information System, pp. 189–203.

Potapov, P., Hansen, M.C., Pickens, A., Hernandez-Serna, A., Tyukavina, A., Turubanova, S., et al., 2022. The global 2000-2020 land cover and land use change dataset derived from the Landsat archive: first results. Front. Remote Sens. 18.

Regasa, M.S., Nones, M., Adeba, D., 2021. A review on land use and land cover change in Ethiopian basins. Land 10 (6), 585.

Shen, X., Liu, B., Henderson, M., Wang, L., Jiang, M., Lu, X., 2022a. Vegetation greening, extended growing seasons, and temperature feedbacks in warming temperate grasslands of China. J. Clim. 1–51.

Shen, X., Liu, Y., Liu, B., Zhang, J., Wang, L., Lu, X., Jiang, M., 2022. Effect of shrub encroachment on land surface temperature in semi-arid areas of temperate regions of the Northern Hemisphere. Agric. For. Meteorol. 320, 108943.

Sisay, G., Gitima, G., Mersha, M., Alemu, W.G., 2021. Assessment of land use land cover dynamics and its drivers in bechet watershed upper blue Nile basin, Ethiopia. Remote Sens. Appl.: Society Environ. 24, 100648.

Tefera, M.M., 2011. Journal of sustainable development in Africa (volume 13, No.1, 2011). J. Sustain. Dev. Afr. 13 (1).

Teferi, E., Bewket, W., Uhlenbrook, S., Wenninger, J., 2013. Understanding recent land use and land cover dynamics in the source region of the Upper Blue Nile, Ethiopia: spatially explicit statistical modeling of systematic transitions. Agric. Ecosyst. Environ. 165, 98–117.

Tewabe, D., Fentahun, T., 2020. Assessing land use and land cover change detection using remote sensing in the Lake Tana Basin , Northwest Ethiopia Assessing land use and land cover change detection using remote sensing in the Lake Tana Basin , Northwest Ethiopia. Cogent Environ. Sci. 6 (1).

Tolessa, T., Dechassa, C., Simane, B., Alamerew, B., Kidane, M., 2020. Land use/land cover dynamics in response to various driving forces in Didessa sub-basin, Ethiopia. Geojournal 85 (3), 747–760.

Turner, W., Rondinini, C., Pettorelli, N., Mora, B., Leidner, A.K., Szantoi, Z., Buchanan, G., Dech, S., Dwyer, J., Herold, M., Koh, L.P., 2015. Free and open-access satellite data are key to biodiversity conservation. Biol. Conserv. 182, 173–176.

Viera, A.J., Garrett, J.M., 2005. Understanding Interobserver Agreement. The Kappa Statistic', Research Series, (May), pp. 360–363.

Woldesenbet, A.B., Wudmatas, S.D., Denboba, M.A., 2020. Enset - Based Land Use Land Cover Change Detection and its Impact on Soil Erosion in Meki River Watershed , Western Lake Ziway Sub - Basin , Central Rift Valley of Ethiopia. Environmental Systems Research [Preprint].

Xu, Y., Dong, K., Jiang, M., Liu, Y., He, L., Wang, J., et al., 2022. Soil moisture and species richness interactively affect multiple ecosystem functions in a microcosm experiment of simulated shrub encroached grasslands. Sci. Total Environ. 803, 149950.

Xu, W., Fan, X., Ma, J., Pimm, S.L., Kong, L., Zeng, Y., Li, X., Xiao, Y., Zheng, H., Liu, J., Wu, B., An, L., Zhang, L., Wang, X., Ouyang, Z., 2019. Hidden loss of wetlands in China. Curr. Biol. 29 (3065–3071), e2.

Yesuph, A.Y., 2020. Prospects of Sustainable Land Management amidst Interlocking Challenges in the Upper Beshillo Catchments , Northeastern Highlands of Ethiopia.

Yesuph, A.Y., Dagnew, A.B., 2019. Land use/cover spatiotemporal dynamics, driving forces and implications at the Beshillo catchment of the Blue Nile Basin, North Eastern Highlands of Ethiopia. Environ. Syst. Res. 8 (1).